

# Generic Contrast Agents

Our portfolio is growing to serve you better. Now you have a *choice*.



[VIEW CATALOG](#)

# AJNR

## **Optimal imaging protocol after intraocular silicone oil tamponade.**

R C Herrick, L A Hayman, R K Maturi, P J Diaz-Marchan, R A Tang and H M Lambert

*AJNR Am J Neuroradiol* 1998, 19 (1) 101-108

<http://www.ajnr.org/content/19/1/101>

This information is current as of May 14, 2025.

# Optimal Imaging Protocol after Intraocular Silicone Oil Tamponade

Richard C. Herrick, L. Anne Hayman, Raj K. Maturi, Pedro J. Diaz-Marchan, Rosa A. Tang, and H. Michael Lambert

**PURPOSE:** Our purpose was to define the optimal protocol for imaging of the orbits after vitreous humor replacement with silicone oil.

**METHODS:** Eleven eyes in 10 patients with tractional and/or rhegmatogenous retinal detachment were studied. Five CT scans and 18 high-field (1.5 T) MR images were obtained. Standard T1-weighted, T1-weighted with fat and silicone saturation, fast spin density-weighted, and T2-weighted orbital MR sequences were performed. Unique pulse sequences included fast spin density-weighted and T2-weighted imaging with and without fat saturation or silicone saturation, gradient-echo imaging, and short-tau inversion recovery imaging.

**RESULTS:** The T1-weighted MR and CT studies were comparable in displaying the silicone. However, the fat- or silicone-saturated fast T2-weighted sequences always showed the fibrous bands and subretinal fluid to best advantage. In one case, the eye also contained inadvertently retained perfluorocarbon liquid, which blended with silicone oil on both saturated images, requiring companion T1-weighted sequences without saturation to demonstrate its presence.

**CONCLUSION:** Simple, commonly available fat-saturated fast T2-weighted MR images supplemented by standard T1-weighted images are all that are needed to evaluate the eye efficiently after vitrectomy and tamponade.

As many as 1% of the population in the United States will have retinal detachment caused by a retinal tear (1). The natural course of this disorder and its treatment are summarized in Figure 1. In the majority of patients, indirect ophthalmoscopy affords an adequate appraisal. However, if there is significant corneal or lens opacification, sonography is useful for identifying the intraocular anatomy. The presence of silicone itself occasionally makes both clinical and sonographic evaluation difficult, and computed tomography (CT) or magnetic resonance (MR) imaging may be required in these cases. In some patients, incidental images of the postoperative eye may be required. The interpretation of these CT or MR studies requires a knowledge of the disease and a familiarity with the agents used for treatment, such as scleral buckles, tamponade with gases, silicone oil, or perfluorocarbon liquid (PFCL).

The appearance of silicone oil and PFCL has been described in standard clinical MR and CT protocols (2–8). Some authors have advocated the addition of a specialized T1-weighted silicone saturation pulse sequence to eliminate chemical-shift artifacts at the silicone oil–aqueous interface (7). In this article, we consider the possible value of fat- or silicone-saturated fast T2-weighted or spin density-weighted MR studies and review our experience with CT and MR imaging after vitreous replacement with silicone oil.

## Methods

A retrospective review was performed of the imaging studies and medical records of 11 patients who underwent 12 vitrectomy procedures followed by silicone oil tamponade for tractional and/or rhegmatogenous retinal detachment. Patients' ages, sex, diagnoses, and the type of surgical procedure they underwent were noted from medical records. In addition, the interval between surgery and imaging was determined. Eighteen MR images and five CT scans were acquired in the 11 patients (12 eyes) after silicone oil tamponade. In six patients, intraoperative PFCL was used. In nine patients, the procedure was a repeat operation. The Table presents a summary of the imaging and clinical data for all 11 patients.

The study group consisted of five men and six women ranging in age from 24 to 60 years. The right eye was involved in 10 patients, the left eye in two patients, and one patient had a bilateral procedure. The interval between operation and imaging was 7 to 489 days (mean, 141 days). Four patients had more than one postoperative imaging study.

Received February 27, 1997; accepted after revision June 9.

Presented in part at the annual meeting of the American Society of Neuroradiology, Seattle, Wash, June 1996.

From the Departments of Radiology (R.C.H., L.A.H., P.J.D.-M.) and Ophthalmology (R.K.M., H.M.L.), Baylor College of Medicine, Houston, Tex; and the Department of Ophthalmology, University of Texas Medical Branch, Galveston (R.A.T.).

Address reprint requests to Richard C. Herrick, PhD, Baylor College of Medicine, Department of Radiology, One Baylor Plaza, Houston, TX 77030.

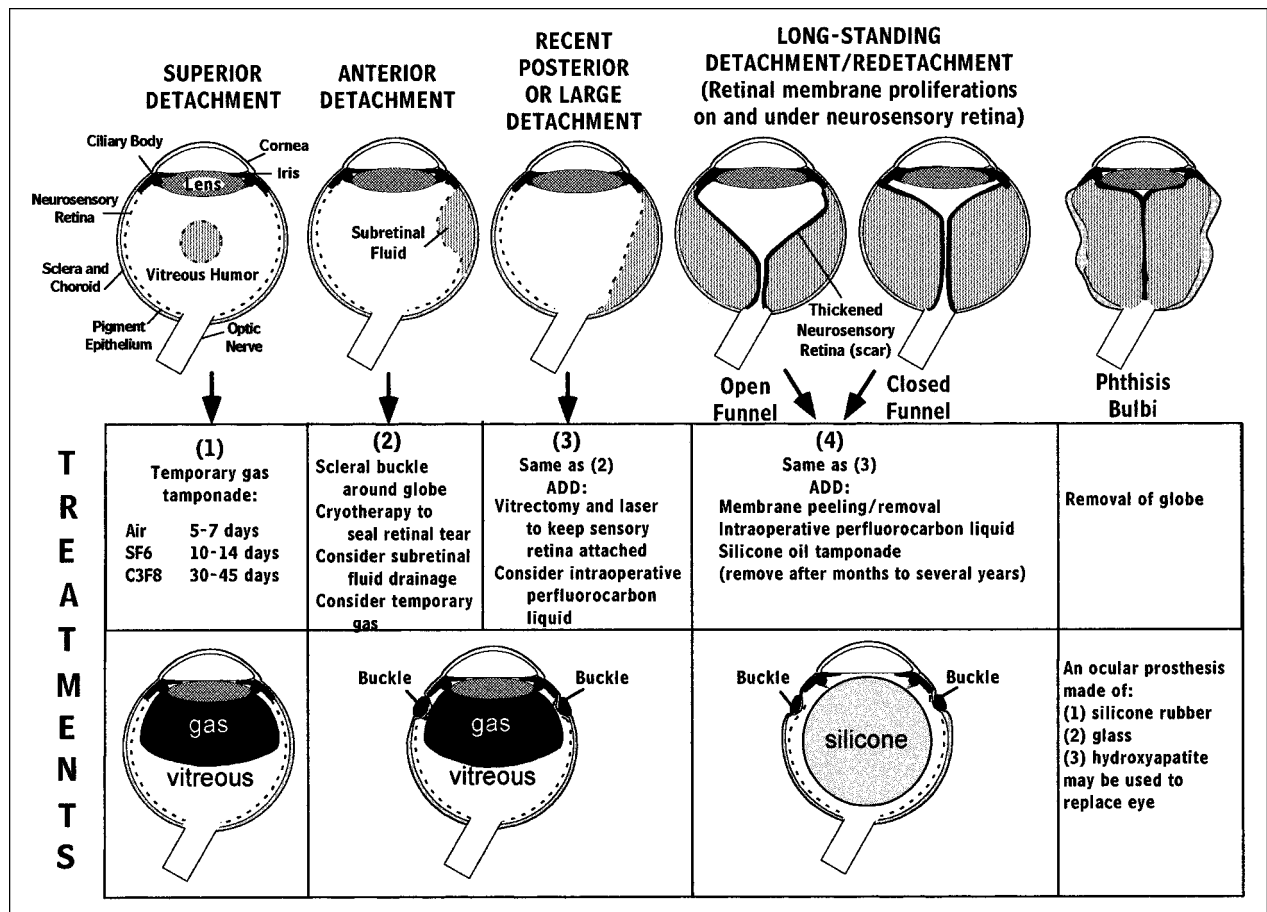


Fig 1. Natural course and treatment of retinal detachments (separation of retinal neurosensory layer from pigment epithelium of retina). The two layers of the retina are the neurosensory (dotted lines) and the retinal pigmented epithelium (RPE, adjacent solid line). Both continue anteriorly into the ciliary body. Posteriorly, the neurosensory retina inserts at the optic nerve while the RPE forms an oval opening at the base of the optic nerve. A tear in the neurosensory layer with associated traction allows fluid to accumulate between these layers, thereby causing retinal ischemia and disrupting retinal function in these areas. Therapeutic attempts to reattach the layers include filling the vitreous cavity with a tamponading agent or decreasing the circumference of the globe with a scleral band. In advanced disease, scar tissue can form in the vitreous cavity (proliferative vitreoretinopathy), making reattachment of the layers more difficult. End-stage disease can result in a shrunken globe (phthisis bulbi), which may be removed for cosmetic reasons or for pain control.

MR imaging was performed postoperatively with a Signa 1.5-T unit (GE Medical Systems, Milwaukee, Wis). The pulse sequences used for each patient are shown in the Table. In general, T1-weighted (500/15/2 [repetition time/echo time/excitations]) spin-echo images and T2-weighted (2000/114) fast spin-echo images were obtained with and without silicone saturation. Silicone saturation was achieved by using standard fat saturation with the frequency offset changed to -290 Hz from the default fat-saturation setting of -220 Hz.

Nine patients (10 eyes) were examined with orbital coils. Two patients (two eyes) were examined with the head coil. A 12- or 16-cm field of view was used in all cases. A 3-mm section thickness was obtained with a 0.5-mm gap in 10 cases (11 eyes) and one patient was examined with no intersection gap. A 256 × 256 matrix was used for all studies except for the T1-weighted images, which were obtained with a 256 × 192 matrix. Gradient-echo and short-tau inversion recovery (STIR) sequences were each used in two patients.

To identify chemical-shift artifacts, a subset of four patients had presaturation sequences obtained with the read/phase-encode axes reversed or with a different bandwidth. The frequency-encoding direction was left to right in six cases (seven eyes) and anterior to posterior in 10 cases (11 eyes). Spin density-weighted images with and without silicone saturation were obtained in three patients.

## Results

Silicone oil showed an unexplained apparent decrease in volume in one patient (P.C.) between 7 and 162 days postoperatively. In two patients, the retina redetached postoperatively, as confirmed by follow-up studies and ophthalmoscopic examination.

STIR sequences were found to be ineffective in nulling silicone oil signal, because the relaxation properties of this substance are different from those of fat; imaging time was also excessive. T2\*-weighted gradient-echo imaging was tried in two cases. It was performed in patient M.W. because presence of blood was suspected on a previous imaging study. In patient G.K., this sequence produced more apparent motion artifacts without providing any additional information than found on the fast T2-weighted sequence.

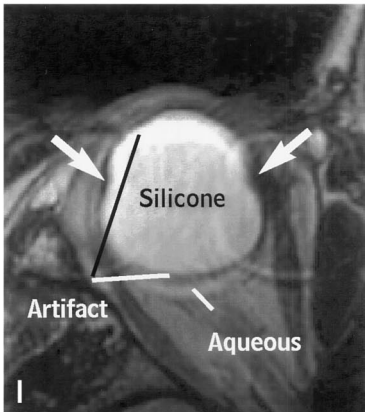
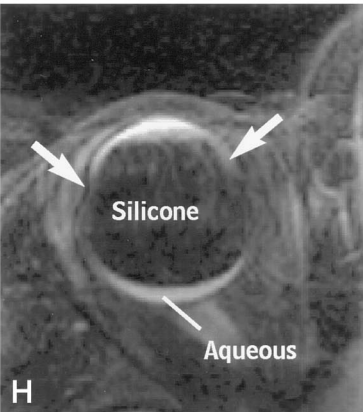
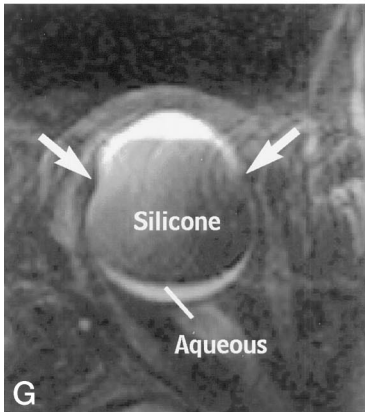
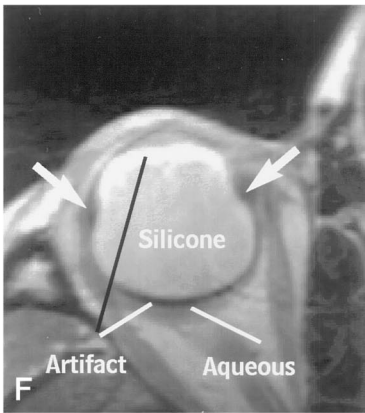
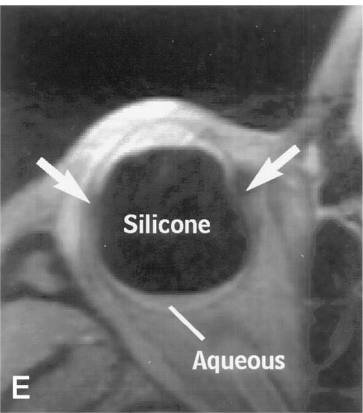
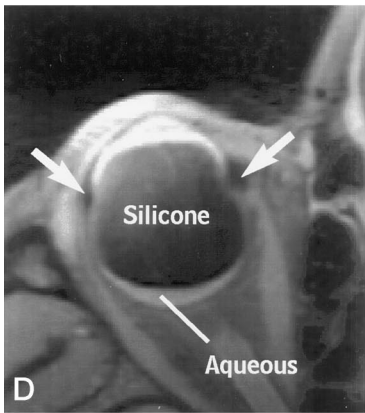
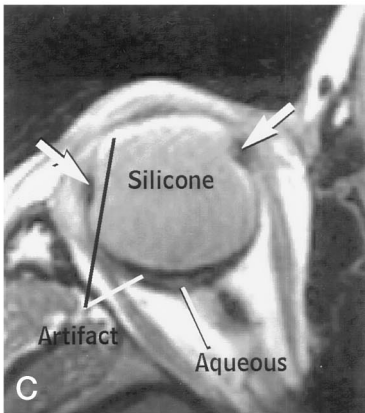
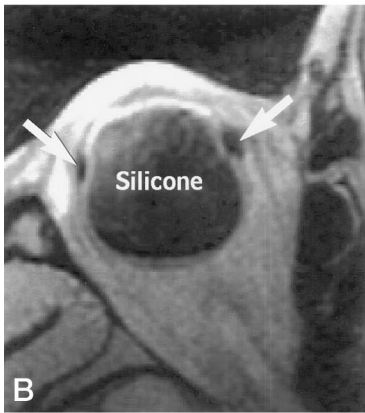
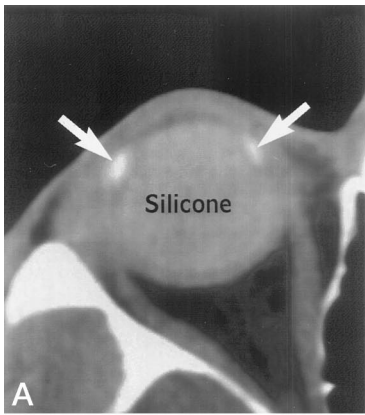
The orbital coils used in nine patients (10 eyes) improved resolution as compared with the head coil used in two patients (two eyes). The frequency-encoding direction from right to left proved to be the

Imaging and clinical data for 11 patients (12 eyes)

Patient	Age, y/Sex	Eye	Diagnosis	Procedure	Interval between Operation and Imaging, d	CT	MR Imaging									Gradient Echo	STIR
							T1-Weighted			T2-Weighted			Spin Density-Weighted				
							Plain	Silicone Saturation	Fat Saturation	Plain	Silicone Saturation	Fat Saturation	Plain	Silicone Saturation	Fat Saturation		
M.W.	49/F	R	RRD, PDR, TRD	PPV, Cryo, RET	29		✓	✓	✓	✓							✓
					214	✓	✓	✓	✓		✓	✓		✓			
					489	✓	✓	✓	✓	✓		✓	✓				
I.A.	24/M	R	RRD, PDR, TRD	PPV, MP, PFCL	319		✓	✓		✓	✓						
G.K.	55/M		RRD, PVR, CMV	PPV, MP, PFCL	95		✓	✓	✓	✓							
					143				✓	✓					✓		
					95		✓	✓	✓	✓					✓		
		R	RRD, PVR, CMV	PPV, MP, PFCL	95		✓	✓	✓	✓						✓	
					143				✓	✓						✓	
P.D.	26/M	R	RRD	PPF, MP, PFCL	121		✓	✓	✓	✓							
L.G.	30/F	R	RRD	PPV, PFCL	74		✓	✓		✓	✓						
					266		✓		✓	✓		✓					
					7		✓	✓		✓	✓						
P.C.	48/F	L	RRD	PPV, SB, Sr, Cryo	7		✓	✓	✓	✓							
					162		✓	✓	✓		✓						
H.S.*	44/M	R	RRD	PPV, PFCL	...	✓	✓	✓	✓							✓	
V.M.	45/M	R	RRD granuloma	PPV, MP, PFCL	110		✓	✓	✓	✓	✓	✓	✓		✓		
F.G.	47/F	R	RRD	PPV, MP	33	✓	✓	✓	✓	✓	✓	✓			✓		
D.V.	60/F	R	TRD, MF	PPV, PPL, MP, EL	43	✓	✓	✓	✓	✓	✓						
D.M.	33/F	R	RRD	PPV, AFX, EL, SB	52	✓	✓	✓	✓	✓	✓	✓	✓	✓			

Note.—AFX indicates air-fluid exchange; CMV, cytomegalovirus; Cryo, cryotherapy; EL, endolaser; Fat, fat saturation; MF, massive fibrosis; MP, membrane peeling; PDR, proliferative diabetic retinopathy; PFCL, perfluorocarbon; PPL, pars plana lensectomy; PPV, pars plana vitrectomy; PVR, proliferative vitreoretinopathy; RET, retinotomy; SB, scleral buckle; SD, spin density; Sili, silicone saturation; Sr, subretinal fluid drainage; SO, silicone oil; STIR, short-tau inversion recovery; RRD, rhegmatogenous retinal detachment; and TRD, tractional retinal detachment.

\* Postoperative referral





optimal way to keep the chemical-shift interface artifacts from distorting the structural features of the anterior and posterior globe (Fig 2).

Figure 2 shows the CT and MR studies of a patient with an uncomplicated postoperative course following silicone oil tamponade. This case is representative of nine of the subjects in the study. In Figure 3, MR and CT studies show a postoperative complication involving redetachment of the retina. Figure 4 shows a serious intraoperative complication with retained PFCL.

### Discussion

The optimal imaging protocol for examining patients after treatment of retinal detachment must define residual scars and subretinal fluid accumulations as well as differentiate tamponade materials. In the following sections we describe the pathologic anatomy and the physical properties of substances used for tamponade (ie, silicone, PFCL, and gas) as well as the advantages and disadvantages of each imaging technique.

#### *Pathologic Anatomy*

The optimal imaging protocol for evaluating the postoperative eye must display the features that have clinical significance. The reoccurrence of detachment (see Figs 1 and 3) necessitates reoperation, especially if it is in the macular area of central vision. CT scans and T1-weighted MR images readily show the position of the silicone oil but do not convey any information about aqueous fluid (Fig 2) or the retinal detachment itself (Fig 3).

The characteristic funnel-shaped retinal detachment is readily observed on fast spin density- and T2-weighted images, with contrast between fluid and scar tissue greatest on the fast T2-weighted sequence (see Fig 3). The unsaturated sequences are somewhat more difficult to interpret, because silicone oil is nearly the same intensity as the subretinal fluid and there is a strong chemical-shift artifact present from the silicone and a less obvious artifact from the orbital fat. The companion fat- or silicone-saturation sequences eliminate the orbital fat and silicone signals and their associated chemical-shift artifacts, improving visibility of the surrounding anatomy. Occasionally, spin density-weighted images are clearer because they have fewer motion artifacts than the T2-

weighted images, owing to the shorter echo time (Fig 2D and G).

#### *Silicone Oil*

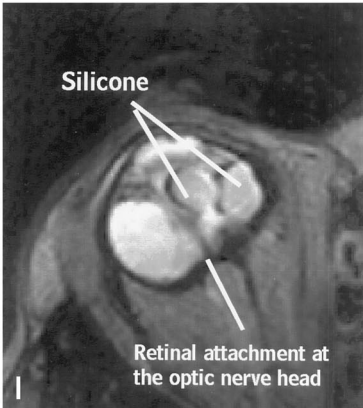
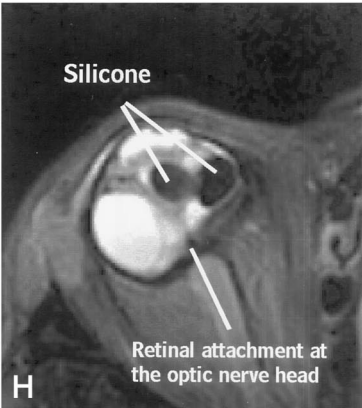
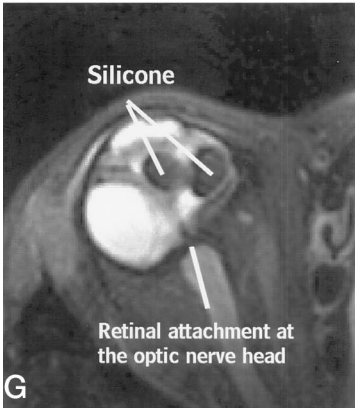
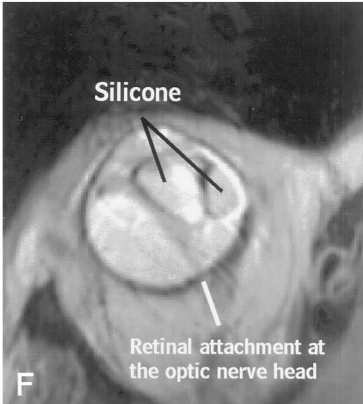
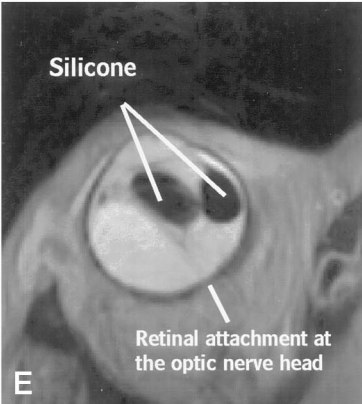
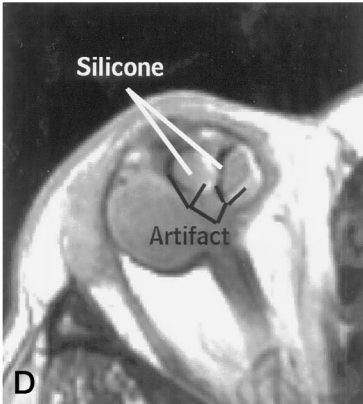
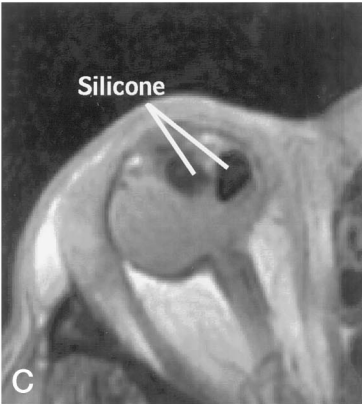
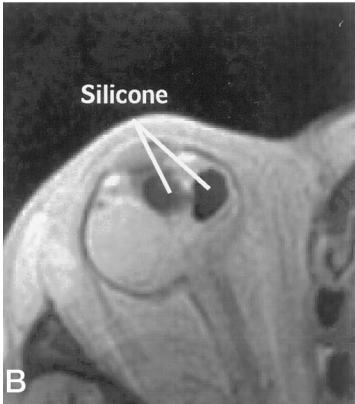
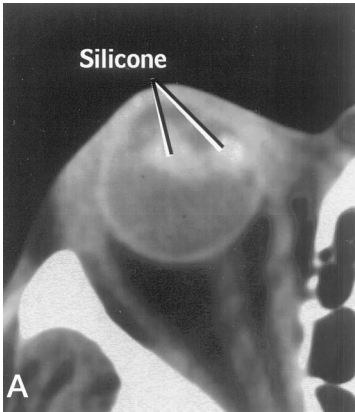
Silicone oils are long polymeric chains of alternating silicon and oxygen atoms with methyl side groups attached to the silicon. In ophthalmology, the term *silicone oil* designates any viscous hydrophobic polymeric compound based on siloxane chemistry. The most commonly used oils are polydimethylsiloxyl and trimethylsiloxyl polymer. The length of the chain determines the oil's viscosity; the greater the length of the polymer, the greater the viscosity of the resulting silicone oil. The stoke is the unit of measure for the ratio of absolute viscosity to density (eg, the viscosity of water is approximately 0.01 stoke or 1 centistoke [cs] at room temperature). Silicone oil in clinical use is actually a mixture of oils of various viscosities, resulting in an average viscosity of 1000 or 5000 cs. Currently, the Food and Drug Administration has approved the use of 5000 cs oil alone because of evidence that it is more stable and causes fewer problems with emulsification in the eye (9). Thus, this higher viscosity is most commonly encountered in the United States, although 1000 cs oil is commonly used in some European countries because it is easier to handle surgically and easier to remove from the eye. At the end of vitrectomy surgery, silicone oil generally appears as a large cohesive droplet filling most of the vitreous cavity. Often, a small quantity of saline used during surgery remains in the eye and appears as a small crescent of fluid between the oil and retinal surface. This fluid is gradually absorbed by the body and replaced by the continually produced aqueous humor.

The appearance of intraocular silicone oil has been described on MR images in 25 cases and on CT scans in 14 cases (3–8). Silicone oil is always hyperdense with respect to contralateral vitreous on CT scans because of the presence of silicon atoms. It is very hyperintense relative to the contralateral normal vitreous on T1-weighted MR images. Silicone has been reported to be hyperintense on spin density- and T2-weighted images by some investigators (4, 6, 8) and isointense on spin density-weighted images and slightly hypointense on T2-weighted images by others (5, 7). This discrepancy is probably due to differences in the viscosity of the oil and in the imaging parameters selected (5). Since T1 and T2 weighting depend

Fig 2. Patient D.M.: imaging examination 52 days after treatment with intraocular silicone oil depicts an uncomplicated postoperative course.

A, Axial CT scan shows hyperdense silicone oil filling the eye, absence of the lens, and eye deformity caused by a solid silicone scleral buckle (arrows).

B–I, Companion axial MR studies, arranged by weighting (rows) and by saturation technique (columns). Note that the collection of aqueous below the silicone oil can only be seen on some of the MR images. B and C are T1-weighted (500/11/2) images, D–F are spin density-weighted (3000/17/2) images, and G–I are T2-weighted (3000/105/2) images. B, D, and G are fat saturated; E and H are silicone saturated; and C, F, and I are without saturation. The best depiction was on the fast spin density-weighted (D) or T2-weighted (G) images with fat saturation. The scans obtained without saturation techniques (C, F, and I) show the characteristic interface artifact (ie, crescent-shaped bright signal on one side of the eye and dark signal on the opposite side). This artifact can be produced on the temporal and nasal sides of the eye or in the anterior and posterior aspects of the eye by selecting different read/phase-encoding directions. The saturated sequences (D, E, G, and H) minimize this artifact and produce excellent visualization of the aqueous layer between the silicone oil and the normal retinal surface. The T1-weighted fat-saturated image (B) in this case did not depict the thin layer of aqueous humor.



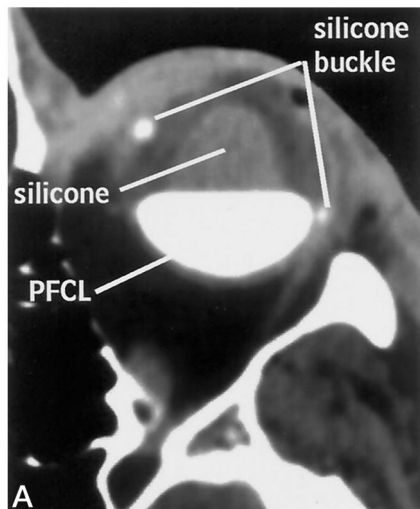
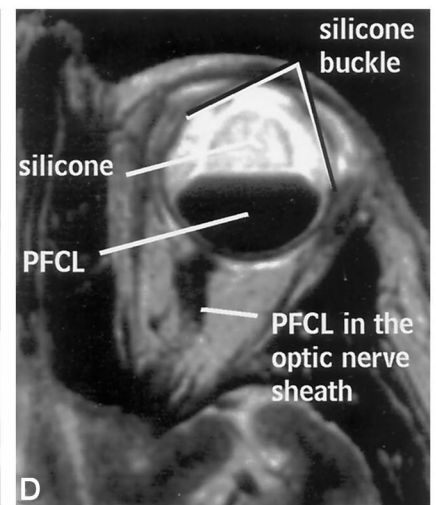
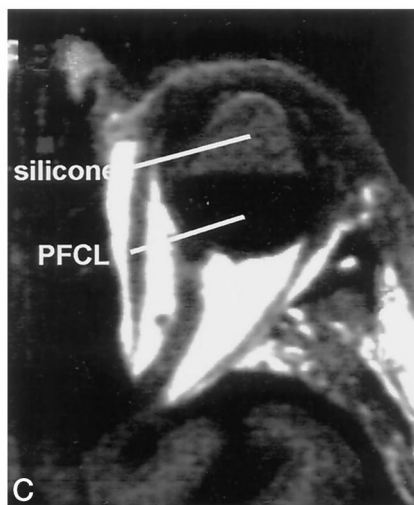
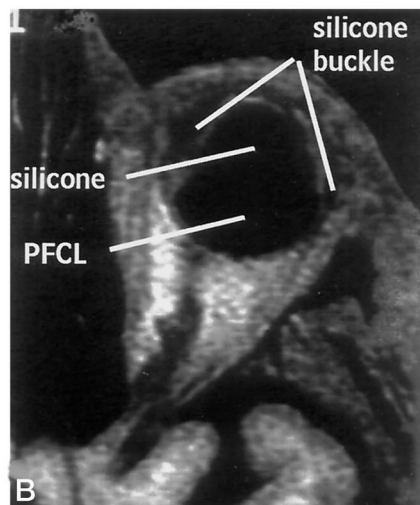


FIG 4. Patient H.S.: imaging examination shows symptomatic silicone oil tamponade with inadvertently retained PFCL.

A, Axial CT scan shows absence of the lens and hyperdense PFCL layering below the less-dense silicone oil in the left eye. A silicone buckle deforms the eye.

B–D, MR images show the expected absence of signal from the perfluorocarbon and silicone buckle. The T1-weighted (800/14/4) fat-saturated image (B) suppresses most of the silicone oil signal and makes it impossible to distinguish residual PFCL from silicone oil. This disadvantage is overcome by consulting the routine T1-weighted (500/14/4) and T2-weighted (2000/80/2) images (C and D, respectively). Extension of PFCL into the nerve sheath is best shown on the T2-weighted image (D).



on the tumbling rate of the oil molecules (which is proportional to the viscosity of the oil), they both depend on oil viscosity. This is particularly true of T2 weighting, which will decrease as viscosity increases. This means that higher-viscosity oils will appear hypointense on a T2-weighted image compared with lower-viscosity oils, and hypointense to a lesser extent on a spin density-weighted image.

In this study, the silicone oil was very hyperdense compared with normal vitreous on CT scans and hyperintense on T1-weighted MR images as compared with vitreous in the contralateral eye. Subtle

contrast changes could not be reliably compared with those in the opposite eye on fast spin density- and T2-weighted images, because the shading artifact from the surface coil decreased the signal across the normal vitreous.

We found the CT and MR studies equally useful in depicting the presence of silicone tamponade (Figs 2–4). All MR pulse sequences showed the expected strong chemical-shift artifacts (ie, dark and bright crescent-shaped bands at the oil-aqueous interface) (Figs 2 and 3). These are prominent because the hydrogen atoms in the silicone oil have a stronger

FIG 3. Patient M.W.: imaging examination 214 days after surgery shows silicone with scarring and open-funnel retinal detachment.

A, Axial CT scan shows absence of the lens and two bubbles of hyperdense silicone oil. The presence of the large bilateral subretinal fluid collections cannot be assessed without consulting the companion MR images, arranged by pulse sequence and saturation technique, as in Figure 2.

B–I, Axial MR images show the capabilities of each pulse sequence. B–D are T1-weighted (500/14/2) images E and F are spin density-weighted (3000/21/2) images, and G–I are T2-weighted (3000/108/2) images. B and G are fat saturated; C, E, and H are silicone saturated; and D, F, and I are without saturation. Note the axial T1-weighted series (B–D) conveys no more information than the CT scan. The spin density-weighted series (E and F) has less contrast than the fast T2-weighted series (G–I). Without saturation techniques, the signal from the silicone can be distinguished from the subretinal fluid only by the artifacts it creates (dark and light bands on either side of the bubbles). The silicone- or fat-saturation pulses create a silicone signal void (B, C, E, G, and H). In this case, either saturation technique produced excellent depiction of the characteristic open funnel-shaped retinal detachment and scar tissue, which separated the neurosensory retina from the large areas of subretinal fluid. The T2-weighted series (G and H) shows greater contrast between scar tissue and subretinal fluid than the spin density-weighted series (E and F).



chemical shift than orbital fat. Silicone has a distinct resonance, which is approximately 290 Hz lower than the water resonance at 1.5 T (lipid hydrogen atoms in orbital fat resonate at 220 Hz lower than water).

Standard fat saturation uses a radio frequency (RF) pulse selectively tuned to the lipid frequency to selectively saturate the lipid signal while leaving the water signal unaffected. Silicone saturation is achieved by changing the RF fat-saturation pulse frequency offset from -220 Hz to -290 Hz. On a GE Signa scanner, the RF pulse saturates a band of frequencies 75 Hz to either side of the fat resonance, so it is understandable that standard fat suppression also gives some degree of silicone suppression. Although maximum suppression of silicone signal was achieved for silicone saturation (when the offset frequency was changed to -290 Hz), fat saturation also provided adequate suppression of the silicone signal (Figs 2 and 3). However, this may not be the case for other scanners, which may use a narrower bandwidth or different pulse shape for their fat-saturation pulse.

### *Intraoperative Perfluorocarbon Liquids*

PFCL compounds include perfluoro-*N*-octane, perfluorophenanthrene, and perfluorodecalin. They appear dark on all MR images because fluorine atoms have been substituted for all the hydrogen atoms in these compounds. On CT scans, the large number of fluorine atoms causes PFCL to appear very hyperdense relative to the vitreous. PFCLs are not normally encountered in imaging because they are removed after intraoperative use to prevent retinal toxicity. When they are inadvertently retained, they layer below the silicone oil, because PFCL is denser than silicone oil. Several in vivo imaging studies of intraocular PFCL have been reported (2, 6), and Girardot et al (3) described its in vitro CT and MR appearance.

In our series, retained PFCL was seen in only one of the six cases in which it was used (Fig 4), in a patient who was referred from another hospital. The absence of signal from PFCL on an MR image caused it to be indistinguishable from the suppressed signal of silicone oil on a fat- or silicone-saturation sequence. Therefore, it is essential to obtain a standard T1-weighted sequence without suppression to detect any inadvertent retention of PFCL.

### *Gases*

Gases are used to provide a short-term intraocular tamponade. The most commonly used gases are air, SF<sub>6</sub>, and C<sub>3</sub>F<sub>8</sub> (see Fig 1). Serial examinations show changes in the volume of these gases as they equili-

brate with intravascular gas and eventually reabsorb. Because of their low density and absence of hydrogen atoms, gases can be optimally detected by their dark appearance on either CT scans or MR images. Although gas and PFCL are both dark on MR imaging sequences, they can readily be distinguished because the relatively low density of gas causes it to rise above the silicone oil, whereas PFCL sinks below the silicone oil. No examples of retained gas were present in our series of patients.

### **Summary**

Both CT and MR imaging are able to illustrate tamponade materials (gas, silicone oil, and inadvertently retained PFCL). However, only one combination of MR sequences was able to define fibrous bands and subretinal fluid accumulations optimally and to distinguish silicone oil from PFCLs. This examination was a silicone- or fat-saturated fast T2-weighted sequence supplemented by a standard T1-weighted pulse sequence.

### **Acknowledgments**

We thank Keith A. Bourgeois, Department of Ophthalmology, University of Texas Health Science Center, Houston, for clinical insights that were very helpful in interpreting our cases, and Brenda Schubert for technical assistance in preparing the manuscript.

### **References**

1. Hilton GF, McLean EB, Brinton DA. **Retinal detachment: principles and practice.** In: *Ophthalmological Monographs*. 5th ed. San Francisco, Calif: American Academy of Ophthalmology; 1989
2. Gewiese BKO, Noske W, Schilling AM, Stiller DA, Wolf KJ, Foerster MH. **Human eye: visualization of perfluorodecalin with F-19 MR imaging.** *Radiology* 1992;185:131-133
3. Girardot C, Hazebroucq VG, Fery-Lemonnier E, et al. **MR imaging and CT of surgical materials currently used in ophthalmology: in vitro and in vivo studies.** *Radiology* 1994;191:433-439
4. Gross JG, Hesselink JR, Press GA, Goldbaum MH, Freeman WR. **Magnetic resonance imaging in the evaluation of vitreoretinal disease in eyes with intraocular silicone oil.** *Am J Ophthalmol* 1990;110:366-370
5. Lidov MW, Maldjian J, Glajchen N, Som PM. **MR appearance of intraocular silicone oil.** *J Comput Assist Tomogr* 1994;18:131-132
6. Manfre L, Fabbri G, Avitabile T, Biondi P, Reibaldi A, Pero G. **MRI and intraocular tamponade media.** *Neuroradiology* 1993;35:359-361
7. Mathews VP, Elster AD, Barker PB, Buff BL, Haller JA, Greven CM. **Intraocular silicone oil: in vitro and in vivo MR and CT characteristics.** *AJNR Am J Neuroradiol* 1994;15:343-347
8. Murray JG, Gean AD, Barr RM. **Intraocular silicone oil for retinal detachment in AIDS: CT and MR appearances.** *Clin Radiol* 1996;51:415-417
9. Heidenkummer H, Kampik A, Thierfelder S. **Experimental evaluation of in vitro stability of purified polydimethylsiloxanes (silicone oil) in viscosity ranges from 1000 to 5000 centistokes.** *Retina* 1992;12:S28-S32